WILEY-VCH

FULL PAPER

A general route to metal-substituted dipnictenes of the type $[L(X)M]_2E_2$ (M = Al, Ga; E = As, Bi; X = halide, amide)

Lars Tuscher,[a] Christoph Helling,[a] Christoph Wölper,[a] Walter Frank,[b] Anton S. Nizovtsev,[c,d,e] and Stephan Schulz*[a]

Abstract: Two equivalents of LGa {L = HC[C(Me)N(2,6-*i*Pr$_2$C$_6$H$_3$)]$_2$} react with PX_3 (X = Cl, Br) with insertion into two P-X bonds and formation of $[L(X)Ga]_2PX$ (X = Cl **1**, Br **2**), whereas the analogous reaction with $AsCl_3$ occurred with twofold insertion and subsequent elimination of $LGaCl_2$ and formation of the Ga-substituted diarsene $[L(Cl)Ga]_2As_2$ (**3**). Analogous findings were observed in the reactions with Me_2NAsCl_2, yielding the unsymmetrically-substituted diarsene [L(Cl)Ga]As=As[Ga(NMe$_2$)L] (**4**). The reaction of $As(NMe_2)_3$ with LGa gave $[L(Me_2N)Ga]_2As_2$ (**5**) after heating at 165 °C for 5 days, while the reaction with LAl gave $[L(Me_2N)Al]_2As_2$ (**6**) after heating at only 80 °C for 1 day. Finally, two equivalents of LGa reacted with $Bi(NEt_2)_3$ to $[L(Et_2N)Ga]_2Bi_2$ (**7**). **1** - **7** were characterized by NMR spectroscopy (^{1}H, ^{13}C, ^{31}P), elemental analysis and single crystal X-ray diffraction (except **1** and **5**). The bonding situations in **4**, **6** and **7** were analyzed by quantum chemical calculations.

Introduction

Monovalent group 13 diyls LM (M = Al, Ga; L = HC[C(Me)N(2,6-*i*Pr$_2$C$_6$H$_3$)]$_2$}) containing an N,N-chelating β-diketiminate ligand exhibit bifunctional properties due to the presence of an electron lone pair, which render these molecules rather Lewis basic, and a formally vacant π-orbital, according to which they show a Lewis acidic character. They therefore act as nucleophiles, i.e., in coordination chemistry, but also show electrophilic reactivity, and this unique reactivity has led to several applications in synthetic chemistry, in particular in the activation of small molecules.[1] Despite their structural analogy, the electronic structure of monovalent LAl and LGa slightly differs. Both show sp-like hybridized, doubly occupied HOMOs and π*-like LUMOs localized at the C-N unit of the ligand. The empty metal p-orbitals in both compounds are the LUMO+1. Quantum chemical calculations revealed that the singlet−triplet energy gap (Al: 34.3−45.7 kcal/mol; Ga: 51.7−55.5 kcal/mol) as well as the HOMO-LUMO separation (Al: 75.76 kcal/mol; Ga 96.24 kcal/mol) in LAl is smaller than in LGa.[2] In addition, LAl and LGa display somewhat different chemical reactivity. The chemistry of LAl mainly focused on bond activation reactions, e.g. small molecule activation (P_4, O_2, S_8, azobenzene, azides)[3] as well as H-X (X= H, Si, B, Al, C, N, P, and O),[4] C-F and C-O bond activation,[5] whereas their use as ligand in coordination chemistry is rather limited. In contrast, LGa has been widely applied as terminal ligand in transition metal complexes,[6] whereas its activity in bond activation reactions of unsaturated organic molecules is rather limited, most likely resulting from the more weakly reducing character of LGa compared to LAl. However, LGa was found to insert into E-X bonds of various elements including H-H, N-H and O-H bonds.[7] Of particular interest are insertion reactions into E-X bonds of heavier main group element compounds such as GaX_3 (X = Cl, Me),[8] Me_3PbCl, $Pb(OSO_2CF_3)_2$ and $Hg(SC_6F_5)_2$.[9] These reactions also yielded compounds with unusual structures and/or oxidation states, i.e. tin clusters $[L(Cl)Ga]_2Sn_7$ and $[L(Cl)Ga]_4Sn_{17}$, which were formed in reactions with $SnCl_2$,[10] dibismuthenes $[L(RO)Ga]_2Bi_2$ (R = C_6F_5, SO_2CF_3),[11] which resulted from reactions with $Bi(OR)_3$, or low-valent germanium complexes $(LGa)_2Ge_2$ and $(LGa)_2Ge_4$,[12] obtained from reactions of base-stabilized $GeCl_2$ with LGa and LGa/KC_8, respectively.

We recently started to investigate reactions of LM with organoantimony complexes, in which the Sb-X bond energy as well as the formal oxidation states of Sb (+I, +II, +III) were systematically varied. In contrast to reactions of LM with $BiEt_3$, which occurred with insertion of LM into the Bi-C bond,[13] the analogous reaction with antimony trialkyls SbR_3 failed, most likely due to the stronger Sb-C bond. In contrast, reactions of LGa with $Sb(NR_2)_3$ and $SbCl_3$ yielded Ga-substituted distibenes $[L(X)Ga]_2Sb_2$ (X = NMe_2, NMeEt, Cl) containing a central Sb=Sb double bond. These Ga-substituted distibenes were transferred into $[L(X)Ga_2(\mu,\eta^{1:1}\text{-}Sb_4)]$ (X = Cl, NMe_2), the first Sb analogues of bicyclo[1.1.0]butane.[14] Moreover, reactions of LM (M = Al, Ga, In) with distibines R_4Sb_2 (R = Me, Et) occurred with insertion of LM into the Sb-Sb bond and formation of $LM(SbEt_2)_2$.[15] Comparable findings were reported for reactions of LAl with diphosphines,[16] whereas the reaction of LGa with $[Cp^*Sb]_4$, in which the Sb atoms adopt the formal oxidation state +I, yielded $[(LGa)_2(\mu,\eta^{2:2}\text{-}Sb_4)]$.[17] Interestingly, analogous reactions with the stronger reducing Mg(I) reagents $[L'Mg]_2$ occurred with formation of $[(LMg)_4(\mu_4,\eta^{2:2:2:2}\text{-}Sb_8)]$ and $[(L'Mg)_4(\mu_4,\eta^{2:2:2:2}\text{-}Sb_8)]$ {L' = HC[C(Me)N(2,4,6-Me$_3$C$_6$H$_2$)]$_2$},[18] containing the Zintl-type $[Sb_8]^{4-}$ anion, as well as $[(L''Mg)_4(\mu_4,\eta^{1:2:2:2}\text{-}Sb_4)]$ (L'' = *i*Pr$_2$NC[N(2,6-*i*Pr$_2$C$_6$H$_3$)]$_2$) containing a $[Sb_4]^{4-}$ tetraanion, respectively.[17]

[a] M. Sc. L. Tuscher, B. Sc. C. Helling, Dr. C. Wölper, Prof. Dr. S. Schulz
Faculty of Chemistry and Center for NanoIntegration (Cenide), University of Duisburg-Essen, Universitätsstr. 5-7, S07 S03 C30, D-45117 Essen, Germany
Fax: (+) 201-183 3830; E-mail: stephan.schulz@uni-due.de
https://www.uni-due.de/ak_schulz/index_en.php
[b] Prof. Dr. W. Frank
Institute for Inorganic Chemistry and Structural Chemistry, Heinrich Heine University of Düsseldorf; Universitätsstr. 1, 40225 Düsseldorf, Germany
[c] Dr. A. S. Nizovtsev
Nikolaev Institute of Inorganic Chemistry, Siberian Branch of the Russian Academy of Sciences, Academician Lavrentiev Avenue 3, 630090, Novosibirsk, Russian Federation
[d] Novosibirsk State University, Pirogova Street 2, 630090, Novosibirsk, Russian Federation
[e] School of Chemistry, University of Nottingham, University Park, Nottingham NG7 2RD, United Kingdom

Supporting information for this article (experimental details including ^{1}H, ^{13}C NMR, IR spectra and computational details) is available on the WWW under http://dx.doi.org/xxx</.

In order to prove if Ga-coordinated dipnictenes of the type $[L(X)Ga]_2E_2$ (E = P - Bi) are generally accessible by reaction of two equivalents of LM with group 15 complexes EX_3, we systematically investigated reactions of LM with halide- and amide-substituted phosphines, arsines and bismuthines EX_3. These reactions proceeded with formation of the double insertion products $[L(X)Ga]_2EX$, which is stable in case of the reactions with PX_3 (X = Cl, Br), or with subsequent elimination of $LGaX_2$ and formation of Ga-substituted dipnictenes containing As=As and Bi=Bi double bonds. The solid state structures of the compounds were determined by single crystal X-ray diffraction, and their bonding situation was further analyzed in detail by quantum chemical calculations.

Results and Discussion

The reactions of two equivalents LGa with PX_3 (X = Cl, Br) in toluene at ambient temperature occurred with insertion of LGa into two P-X bonds and formation of the stable Ga-coordinated phosphines $[L(X)Ga]_2PX$ (X = Cl **1**, Br **2**), which were isolated as pale green (**1**) and pale yellow crystalline solids (**2**) after workup (Scheme 1). Similar twofold insertion reactions of a germylene in the P-Cl bonds of $(Me_2N)PCl_2$ have recently been reported.[19] In contrast, no reaction was observed for the analogous reaction of LGa with $P(NMe_2)_3$ even at high reaction temperatures up to 125 °C and prolonged reaction times (24 h) in toluene.

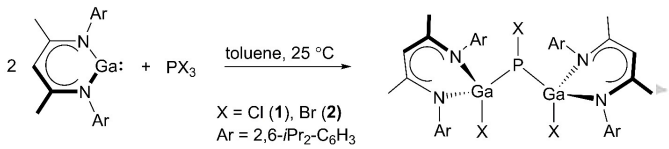

Scheme 1. Synthesis of **1** and **2**.

In contrast, the reactions of two equivalents of LGa with $AsCl_3$ and $As(NMe_2)_3$ occurred with elimination of $LGaCl_2$ and $LGa(NMe_2)_2$, respectively, as was confirmed by ^{1}H NMR spectroscopy (Figure S23) and subsequent formation of the corresponding Ga-substituted diarsenes $[L(Cl)Ga]_2As_2$ (**3**) and $[L(Me_2N)Ga]_2As_2$ (**5**), while the analogous reaction with Me_2NAsCl_2 yielded [L(Cl)Ga]As=As[Ga(NMe$_2$)L] (**4**). In order to identify the reaction mechanism, the *in situ* ^{1}H NMR spectrum of this reaction (Figure S24) was compared with ^{1}H NMR spectra of isolated samples of $LGaCl_2$ and $LGa(NMe_2)_2$ and with an *in situ* ^{1}H NMR spectrum of the reaction of $LGaCl_2$ with one eq. of $LiNMe_2$, which shows three resonances of the backbone C-H moiety indicating the presence of $LGaCl_2$, $LGa(NMe_2)_2$ and a third product, most likely $LGa(Cl)NMe_2$. Comparison of the backbone C-H resonances in these spectra clearly shows that LGa reacts with Me_2NAsCl_2 with elimination of equal amounts of $LGaCL_2$ and $LGa(Cl)NMe_2$, while the formation of $LGa(NMe_2)_2$ can be excluded. In addition, the ^{1}H NMR spectrum neither shows the formation of $[L(Cl)Ga]_2As_2$ (**3**) nor $[L(Me_2N)Ga]_2As_2$ (**5**).

The influence of the substituent on the reactivity of the arsines can clearly be seen, since the reaction of LGa with $AsCl_3$ and Me_2NAsCl_2 occurred smoothly at ambient temperature within minutes, whereas that with $As(NMe_2)_3$ required much harsher reaction conditions and the formation of the corresponding diarsene $[L(Me_2N)Ga]_2As_2$ (**5**) was only finished after heating the solution up to 165 °C for five days (Fig. S22). In contrast, the analogous reaction with LAl yielded $[L(Me_2N)Al]_2As_2$ (**6**) after heating at 80 °C for one day, clearly demonstrating the higher reduction potential of LAl compared to LGa (Scheme 2).

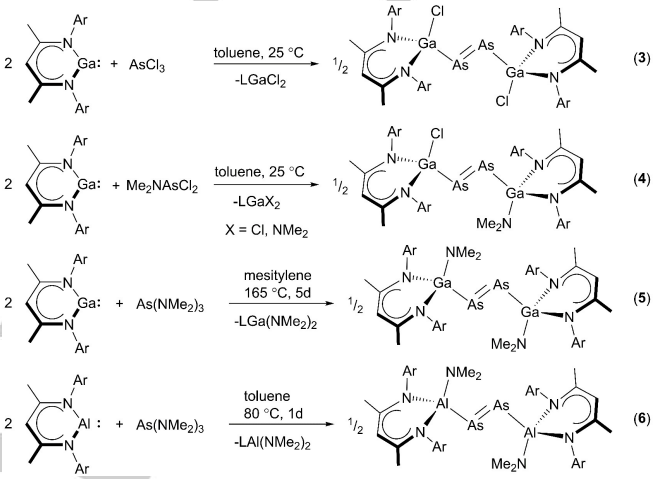

Scheme 2. Synthesis of **3**-**6**.

Finally, the reactions of LGa with several Bi amides were studied (Scheme 3). While the reaction of two equivalents of LGa with $Bi(NMe_2)_3$ only yielded Bi metal and $LGa(NMe_2)_2$ (as confirmed by ^{1}H NMR spectroscopy, Figure S23) even at low temperatures, that with sterically more pronounced $Bi(NEt_2)_3$ gave $[L(Et_2N)Ga]_2Bi_2$ (**7**) in good yields. $[L(Et_2N)Ga]_2Bi_2$ (**7**) was formed at milder reaction conditions (25 °C, 4 days) compared to the diarsene $[L(Me_2N)Ga]_2As_2$ (**5**), which clearly results from the weaker Bi-N bond compared to the As-N bond. It should further be mentioned that the analogous reaction of LGa with $Sb(NMeEt)_3$ required heating at 60 °C in the absence of any solvents for seven days, whereas the reaction with the sterically less hindered $Sb(NMe_2)_3$ proceeded already very slowly at ambient temperature, but is finished after heating to 75 °C for 24 h.[14] In contrast, no reaction between LGa and the sterically more demanding $Sb(NEt_2)_3$ was observed, even after prolonged heating at 120 °C. Analogous trends were observed for the reactions of two equivalents of LGa with ECl_3 (E = As, Sb, Bi). The reaction with $AsCl_3$ occurred at ambient temperature, whereas that with $SbCl_3$ is finished within minutes already at 0 °C. In contrast, the reaction with $BiCl_3$ occurred slowly at ambient temperature with formation of elemental bismuth as well as $LGaCl_2$, but we could not prove if this reaction proceeds via formation of an thermally unstable dibismuthene $[L(Cl)Ga]_2Bi_2$ or if $BiCl_3$ is directly reduced to Bi. However, these experimental findings clearly reveal the strong influence of the strength of the

E-X (X = Cl, N) bond as well as the steric demand of the amido (NR_2) substituent.

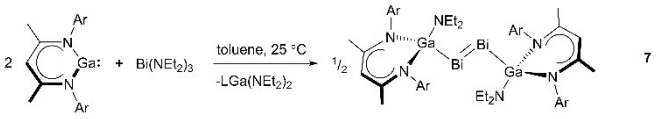

Scheme 3. Synthesis of **7**.

Isolated **1** – **7** are thermally stable and can be stored in a glove box under Ar atmosphere for several months. The thermal stability of the compounds differ significantly. **1**, **2**, **4** and **6** melt without decomposition at 222 °C (**2**), 239 °C (**4**) and 275 °C (**6**), while **3** and **7** decomposes at 255 °C (**3**) and 120 °C (**7**), respectively, without melting.

Solution-phase characterization. **1** and **2** dissolve moderately in benzene, toluene and hexane, whereas **3** - **7** dissolve poorly in benzene and toluene and are insoluble in hexane. The ^{1}H NMR spectrum of **1** and **2** in toluene-d_8 show the expected septets and doublets for the *i*Pr groups of the β-diketiminate ligand as well as single resonances of the γ-CH and two methyl groups of the β-diketiminate ligand (Table 1). These findings are confirmed by the ^{13}C NMR spectrum, which only shows the expected resonances of the β-diketiminate groups. The ^{31}P NMR spectra of **1** and **2** show single resonances at 0.52 (**1**) and -42.9 ppm (**2**), which prove the formation of a phosphine rather than a diphosphene. Diphosphenes of the type R_2P_2[20] and metal-substituted diphosphenes such as [(^{Me}PDI)IrCO]$_2$(μ-P_2) (PDI = pyridine-diimine) and [(silox)$_3$M]$_2$(μ:η^1,η^1-P_2) (M = Nb, Ta) typically exhibit resonances between 440 and 550 ppm.[21] Heating a solution of [L(Cl)Ga]$_2$PCl (**1**) in toluene-d_8 at 125 °C for 5 d resulted in the formation of several new phosphorous species, but the formation of a diphosphene was excluded due to the lack of any resonances in the typical range. However, two new triplets at -187.4 and -338.1 ppm ($^1J_{PP}$ = 140 Hz) in the ^{31}P NMR spectrum (Figure S25), which appear in the typical range for tetraphosphabicyclobutanes R_2P_4,[22] show the formation of [L(Cl)Ga]$_2P_4$ as was previously observed for [L(Cl)Ga]$_2$Sb$_4$.[14] In addition, the *in situ* ^{1}H NMR spectrum shows the formation of $LGaCl_2$ as by-product as was also observed for the formation of [L(Cl)Ga]$_2$Sb$_4$.

The ^{1}H NMR spectra of **3** to **7** are very similar and each show two septets and four doublets for the magnetically inequivalent *i*Pr groups of the *β*-diketiminate ligand as was previously observed for the corresponding distibenes [L(X)Ga]$_2$Sb$_2$ (X = Cl, NMe_2),[14] while the γ-CH and two methyl groups of the C_3N_2M ring exhibit only single resonances. The ^{13}C NMR spectra of **1**, **2**, **3** and **6** show the expected 15 resonances of the β-diketiminate groups, whereas unsymmetrical **4** shows only 29 of the expected 30 resonances of the β-diketiminate groups (Figure S13) and two additional resonances of the NMe_2 group. However, the resonance at 24.8 ppm appears with twofold intensity, indicating an overlap of two signals, which is supported by the fact that only 7 resonances instead of eight are observed for the *i*Pr groups.

1 - **4** and **6** are stable in toluene solutions and don't show any kind of decomposition up to temperatures of 80 °C. A solution of **7** in toluene also doesn't show any sign of light sensitivity and can be stored for weeks at ambient temperature without decomposition, whereas it decomposes gradually at elevated temperatures even in the dark with precipitation of Bi metal and formation of unidentified reaction products.

Table 1. ^{1}H NMR chemical shifts of **1 - 4**, **6** and **7**.[a]

	γ-C*H*	C*H*Me$_2$	CH*Me*$_2$	C*Me*	N*R*$_2$
1[b]	4.81	3.55, 3.22	1.21, 1,18, 0.98	1.46	---
2[b]	4.87	3.63, 3.24	1.25, 1.20, 0.96	1.47	---
3[b]	4.85	3.77, 2.90	1.35, 1.24, 1.09, 0.97	1.61	---
4[b]	4.87, 4.72	3.77, 3.54, 3.17, 2.77	1.31, 1.21, 1.13, 1.02, 0.98, 0.97	1.63, 1.60	2.95, 2.37
6[b]	4.92	3.53, 2.93	1.28, 0.99, 0.96	1.61	2.69, 2.36
7[c]	4.74	2.77, 4.07	1.05, 1.11, 1.29, 1.39	1.58	1.02, 1.36, 2.80, 3.72

[a] NMR spectra of **5** couldn't be recorded due to its poor solubility in organic solvents; [b] in toluene-d_8 , [c] in benzene-d_6

Solid state structures. The molecular structures of **2·2C$_7$H$_8$**, **3**, **4**, **6** and **7** were determined by single crystal X-ray diffraction. Single crystals were obtained from saturated solutions in toluene upon storage at -30 °C for 3 days (**2**), at 0 °C (**3**) or at room temperature for 2 days (**7**) and 3 days (**4** and **6**). **2·2C$_7$H$_8$** crystallizes in the monoclinic space group *P*2$_1$/*c* with the molecule and two disordered toluene molecules in general positions (Figure 1). Since the central P–Br unit is disordered over three positions with the atomic displacement parameters of the corresponding atoms still large, a meaningful quantitative discussion of this part of the molecule is not feasible. The Ga-Br bond lengths (Table 2) of the three disordered units slightly differ. The Ga atoms adopt distorted tetrahedral coordination spheres and the β-diketiminate ligands deviate from planarity as is typical for LGaX fragments.

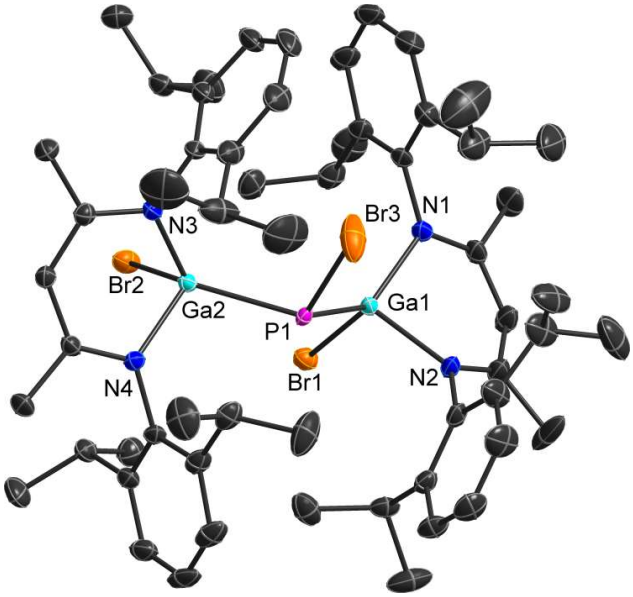

Figure 1. Molecular structure of $[L(Br)Ga]_2PBr$ in the crystal of $\mathbf{2}\cdot 2C_7H_8$. H-atoms and minor components of the disordered PBr and *i*Pr units as well as the disordered solvent molecules were omitted for clarity. Displacement ellipsoids are drawn at the 50% probability level.

The metal-substituted diarsene $[L(Cl)Ga]_2As_2$ (**3**) crystallizes monoclinic with space group $P2_1/n$, while $[L(Cl)Ga]As{=}As[Ga(NMe_2)L]$ (**4**) and $[L(Me_2N)Al]_2As_2$ (**6**) crystallize in the triclinic space group *P*-1 (Figures 2 - 4). **3** and **4** are located on centers of inversion.

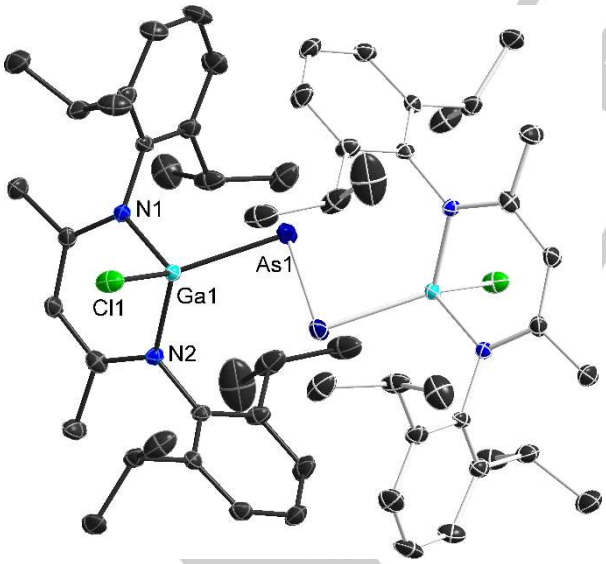

Figure 2. Molecular structure of $[L(Cl)Ga]_2As_2$ in the crystal of **3**. H-atoms were omitted for clarity. Displacement ellipsoids are drawn at the 50% probability level and the symmetry generated part of the molecule is depicted in pale colors (-x, 2-y, -z).

Since the point group symmetry of the molecule of **4** does not match the site symmetry, the Cl and NMe_2 substituents are superimposed. Refinement in a space group of lower symmetry did not yield an acceptable model.

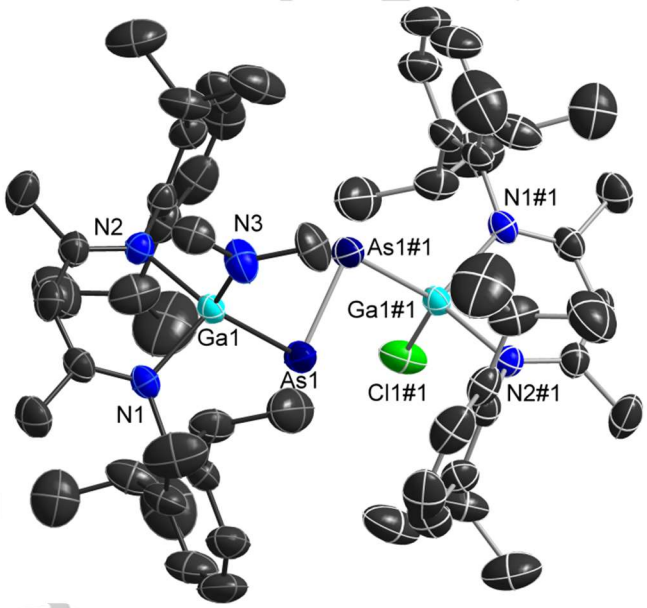

Figure 3. Molecular structure of $[L(Cl)Ga]As{=}As[Ga(NMe_2)L]$ in the crystal of **4**. H-atoms were omitted for clarity. Displacement ellipsoids are drawn at the 50% probability level and the symmetry generated part of the molecule is depicted in pale colors (#1 1-x, 1-y, -z). Cl and the NMe_2 group are disordered by inversion symmetry and only one of the positions is shown.

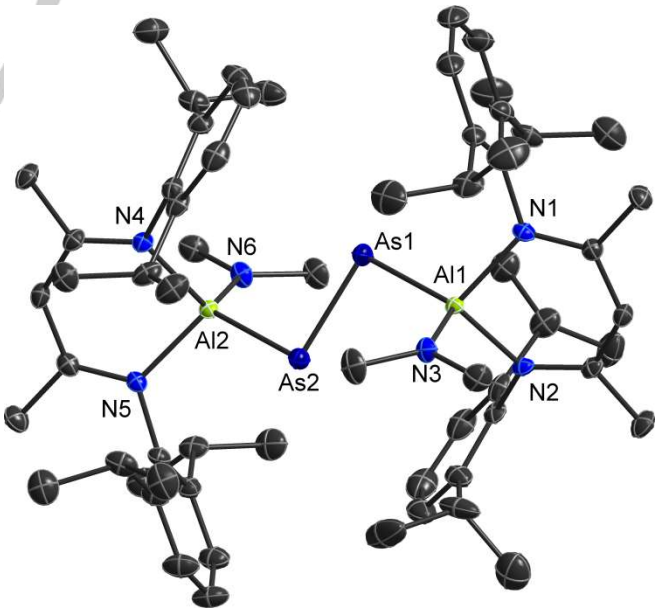

Figure 4. Molecular structure of $[L(Me_2N)Al]_2As_2$ in the crystal of **6**. H-atoms were omitted for clarity. Displacement ellipsoids are drawn at the 50% probability level.

The dibismuthene $[L(Et_2N)Ga]_2Bi_2$ (**7**) crystallizes in the monoclinic space group $P2_1/n$ and is also placed on a center of inversion (Figure 5).

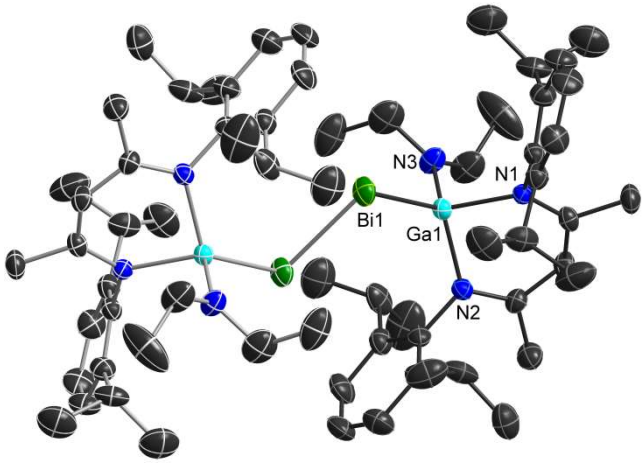

Figure 5. Molecular structure of $[L(Et_2N)Ga]_2Bi_2$ in the crystal of **7**. H-atoms and the minor occupied carbon atom positions of the disordered ethyl group at N3 were omitted for clarity. Displacement ellipsoids are drawn at the 50% probability level and the symmetry generated part of the molecule is depicted in pale colors (symmetry operation 1-x, 1-y, -z).

Compared to the analogous distibene structures $[L(X)Ga]_2Sb_2$ (X = Cl, NMe_2, NMeEt),[14] neither changing M (Al, Ga) nor E (As, Sb, Bi) strongly influences the overall conformation of the molecule. The As atoms in $[L(Cl)Ga]_2As_2$ (**3**), [L(Cl)Ga]As=As[Ga(NMe_2)L] (**4**) and $[L(Me_2N)Al]_2As_2$ (**6**) are slightly further off the plane formed by the ligands' backbones (offset from best plane of the backbones: 0.195(6) Å (**3**), 0.4097(13) Å (**4**), 0.4503(8) and –0.5168(8) Å (**6**), 0.0192(23) Å (**7**)). The As=As bond lengths in **3** (2.2556(6) Å), **4** (2.2554(8) Å) and **6** (2.2707(4) Å) are comparable to those reported for diarsenes of the general type RAs=AsR (2.219 - 2.358 Å; mean bond length 2.271 Å),[23] but shorter compared to the heavier congeners $[L(X)Ga]_2Sb_2$ (X = Cl, NMe_2, NMeEt) and $[L(Et_2N)Ga]_2Bi_2$ (**7**) (2.8132(5) Å). In addition, the E-E bond distances in **3** - **7** are shorter than the sum of the calculated atomic radii [1.21 (As), 1.40 (Sb), 1.51 Å (Bi);[24] 1.31 (As), 1.46 (Sb) , 1.50 Å (Bi)[25]], most likely due to the lower coordination number (c.n. 2) of **3** - **7** compared to the calculated values (c.n. 3).

The Bi-Bi bond length of $[L(Et_2N)Ga]_2Bi_2$ (**7**) matches well with those of $[L(RO)Ga]_2Bi_2$ (R = C_6F_5 2.8182(4) Å; SO_2CF_3 2.8111(2) Å)[11] and other dibismuthenes found in the CSD database (2.796 - 2.893 Å; mean bond length 2.831 Å).[26] However, the Ga-Bi (2.7061(6) Å) and Ga-N1/2 bonds (av. 2.006 Å) in **7** are slightly elongated compared to those in $[L(RO)Ga]_2Bi_2$ (R = C_6F_5: Ga-Bi 2.693(6) Å, av. Ga-N 1.952 Å; SO_2CF_3: Ga-Bi 2.655(1) Å, av. Ga-N 1.928 Å), which can be attributed to the weaker electron-withdrawing nature of the NEt_2 group in $[L(Et_2N)Ga]_2Bi_2$ (**7**) compared to the OR groups in $[L(RO)Ga]_2Bi_2$.

Table 2. Comparison of bond lengths (Å) and angles (°) in **2**, **3**, **4**, **6** and **7**.

	2[a]	**3**	**4**[b]	**6**[c]	**7**[d]
E-E	-	2.2556(6)	2.2554(8)	2.2707(4)	2.8132(5)
M-E	2.346(2) 2.279(2)[e] 2.388(5)[e]	2.3957(5)	2.4217(6)	2.4554(7) 2.4501(7)	2.7061(6)
M-X	2.3550(4) 2.3631(4)	2.2247(8)	2.190(9) (Ga-Cl) 1.84(2) (Ga-N)	1.802(2) 1.806(2)	1.884(5)
M-N_L	1.947(2) 1.967(2) 1.955(2) 1.961(2)	1.936(2) 1.944(2)	1.974(3) 1.978(3)	1.918(2) 1.928(2) 1.921(2) 1.926(2)	2.005(4) 2.006(4)
M-E-E	-	92.69(2)	95.23(3)	95.64(2) 95.69(2)	95.38(2)
Ga-P-Ga	118.94(8) 120.01(8)[e] 114.9(2)[e]	-	-	-	-
N_L-M-N_L	95.99(10) 95.93(10)	96.98(9)	95.28(12)	94.91(9) 94.51(8)	93.39(18)
X-M-E	109.31(7) 121.06(5) 117.40(5)[e] 107.34(5)[e] 118.72(12)[e] 122.62(12)[e]	117.43(3)	118.3(2)	118.69(7) 116.59(7)	114.87(14)
Br-P-M	102.46(10) 104.05(11) 99.97(9)[e] 103.42(8)[e] 110.9(2)[e] 102.7(2)[e]	-	-	-	-

[a] M = Ga, X = Br; [b] M = Ga, X = Cl/NMe_2; [c] M = Al, X = NMe_2; [d] M = Ga, X = NEt_2; [e] 2nd and 3rd component of the disordered part, note that P-Br bond lengths are restrained to be equal; N_L= N of the L ligand.

Quantum chemical calculations. The bonding situations in **4**, **6** and **7** were analyzed by using a number of quantum chemical techniques to gain further insight into the chemical bonding within the M_2E_2 (M = Al, Ga; E = As, Bi) skeletons and also to compare the results with those observed in $[L(X)Ga]_2Sb_2$ (X = Cl, NMeEt).[14] All calculated bond lengths within the M_2E_2 cores (BP86-D3/def2-SVP level of theory,[27–31] Tables S2–S4) are in good agreement with the corresponding experimental values (Δr = 0.01–0.05 Å).

As predicted by atoms in molecules (AIM), electron localization function (ELF), and natural bond orbital (NBO) analyses,[32–35] the E–E bonds in **4**, **6** and **7** are covalent (Tables S2–S4, Figures 6–8), in accordance to reported computational data for pnictogen-containing species.[36]

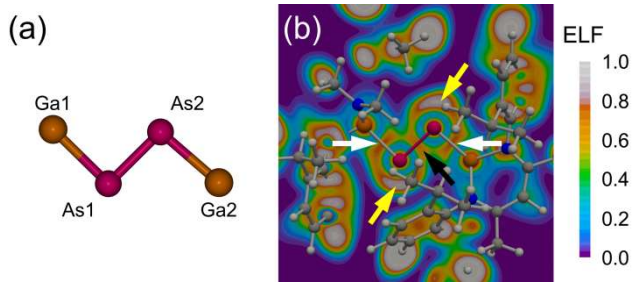

Figure 6. (a) Atomic labelling for the Ga_2As_2 skeleton and (b) ELF distribution in [L(Cl)Ga]As=As[Ga(NMe$_2$)L] (**4**) in the Ga1–As1–As2 plane. V(Ga,As), V(As), and V(As,As) basins are indicated by white, yellow, and black arrows, respectively.

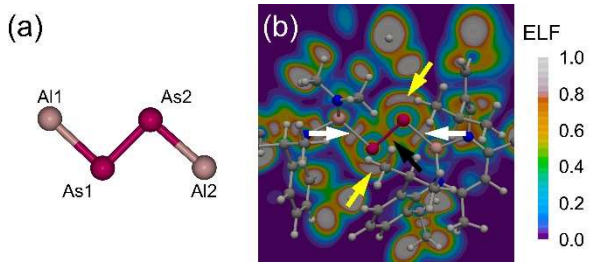

Figure 7. (a) Atomic labelling for the Al_2As_2 skeleton and (b) ELF distribution in [L(Me$_2$N)Al]$_2$As$_2$ (**6**) in the Al1–As1–As2 plane. V(Al,As), V(As), and V(As,As) basins are indicated by white, yellow, and black arrows, respectively.

Moreover, multiple bonding between pnictogen centers is observed for these complexes. Indeed, NBO analysis finds two-center two-electron σ_{E-E} and π_{E-E} bonds with occupation numbers (ON) varying from 1.9 to 2.0 |*e*| (Tables S2–S4) and ELF distribution reveals two disynaptic V(E,E) basins in **4**, **6** and **7** ($\bar{N}$[V(E,E)] = 1.1–1.3; Figures 6–8). Thus, **4** and **6** possess As=As double bonds, whereas **7** contains a Bi=Bi double bond. Additionally, each E atom from **4**, **6** and **7** has one electron lone pair (Tables S2–S4), as calculated by NBO analysis (ON=1.9–2.0 |*e*|) and ELF ($\bar{N}$[V(Sb)] = 2.8–3.0 *e*; Figures 6–8).

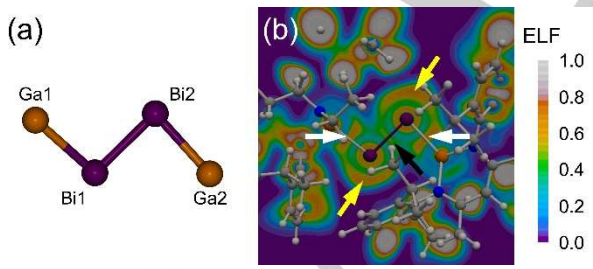

Figure 8. (a) Atomic labelling for the Ga_2Bi_2 skeleton and (b) ELF distribution in [L(Et$_2$N)Ga]$_2$Bi$_2$ (**7**) in the Ga1–Bi1–Bi2 plane. V(Ga,Bi), V(Bi), and V(Bi,Bi) basins are indicated by white, yellow, and black arrows, respectively.

Covalent M–E bonds are characterized by disynaptic V(M,E) basins populated by 2.3–2.4 *e* and σ_{M-E} bond orbitals (ON=2.0 |e|) that are polarized toward the pnictogen end. The polarity of M–E bonds is increased in the order Ga–Bi < Ga–As < Al–As as can be seen from the values of polarization coefficients ($|c_M|^2$; 43–44% > 34–38% > 27–28%), the contributions of the electrons of M into the V(M,E) basins according to ELF/AIM intersection procedure ($\bar{N}$[V(M,E)|M]; 1.2–1.3 *e* > 1.0–1.2 *e* > 0.3 *e*),[37] and the differences between natural population analysis (NPA) partial charges on M and E (Δq; 1.3 |*e*| < 1.4–1.6 |*e*| < 2.0 |*e*|). AIM analysis suggests *shared* Ga–As interactions ($\nabla^2\rho(\mathbf{r}_b)$<0; $|V(\mathbf{r}_b)|/G(\mathbf{r}_b)$>2, $H(\mathbf{r}_b)$<0) and *intermediate* Al–As and Ga–Bi interactions ($\nabla^2\rho(\mathbf{r}_b)$>0; 1<$|V(\mathbf{r}_b)|/G(\mathbf{r}_b)$<2, $H(\mathbf{r}_b)$<0).

It should be noted that the same bonding pattern was observed for Ga_2Sb_2 cores in closely related distibene complexes.[14] Wiberg bond indices (WBIs) calculated for **4**, **6**, **7** as well as [L(Cl)Ga]$_2$Sb$_2$ and [L(MeEtN)Ga]$_2$Sb$_2$ (Tables S2–S4) indicate double and single bond character for all E–E (WBI = 1.8) and M–E (WBI = 0.8–1.0) bonds, respectively, confirming common chemical bonding picture within M_2E_2 units. The energies of frontier molecular orbitals (Figure S22) give HOMO–LUMO gaps ranging between 5.55 (**7**) – 6.27 (**4**) eV. Ionization potentials of [(LMX)$_2$E$_2$] compounds, which can be estimated as –*E*(HOMO) according to Koopmans' theorem, are decreased in the order [L(Cl)Ga]$_2$Sb$_2$ < **4** < [L(MeEtN)Ga]$_2$Sb$_2$ < **6** < **7**.

Conclusions

In summary, reactions of LGa with phosphorus, arsenic and bismuth halides and amides were studied, revealing clear trends in the reactivity as well as different reaction pathways. The reaction of LGa with PX_3 (X = Cl, Br) stopped after twofold insertion into the P-X bonds and formation of [L(X)Ga]$_2$PX (X = Cl **1**, Br **2**), whereas the analogous reactions with $AsCl_3$, Me_2NAsCl_2 and $As(NMe_2)_3$ further proceeded with elimination of $LGaX_2$ (X = Cl, NMe_2) and subsequent formation of the corresponding diarsenes [L(Cl)Ga]$_2$As$_2$ (**3**), [L(Cl)Ga]$_2$As$_2$[Ga(NMe$_2$)L] (**4**), and [L(Me$_2$N)Ga]$_2$As$_2$ (**5**). The reaction of LGa with $As(NMe_2)_3$ required very harsh conditions (165 °C, 5 d), whereas the reaction with stronger σ-donor and stronger reducing agent LAl already proceeded at 80 °C and yielded [L(Cl)Al]$_2$As$_2$ (**6**) after 1 day. Finally, the reaction of LGa with $Bi(NEt_2)_3$ also occurred with insertion and elimination of $LGa(NEt_2)_2$ and formation of the corresponding Ga-substituted dibismuthene [L(Et$_2$N)Ga]$_2$Bi$_2$ (**7**). **2**, **3**, **4**, **6** and **7** were structurally characterized by single crystal X-ray diffraction and the bonding situation, which was investigated by quantum chemical calculations, clearly revealed the double bond character within these complexes.

Experimental Section

General Procedures. The reactions were performed in purified argon atmosphere using standard Schlenk and glove-box techniques. Solvents were dried using a MBraun Solvent Purification System and carefully degassed. Karl Fischer titration of the dry solvents show values less than 3 ppm. Deuterated NMR solvents were stored over activated molecular sieves (4 Å) and degassed prior to use. LGa,[38] LAl,[39] $As(NMe_2)_3$,[40] and

$Bi(NEt_2)_3$[41] were prepared according to literature methods and Me_2NAsCl_2 was prepared by a ligand exchange reaction of $As(NMe_2)_3$ with two equivalents of $AsCl_3$. PBr_3 and $AsCl_3$ were obtained from commercial sources and purified prior to use by distillation or sublimation.

Instrumentation. The ^1H (300, 500 & 600 MHz), $^{13}C\{1H\}$ (75.5, 125 & 150 MHz) and ^{31}P NMR (200 MHz) spectra (δ in ppm) were recorded using a Bruker Avance DPX-300 or Bruker Avance III HD spectrometer and the spectra were referenced to internal C_6D_5H (^1H: δ = 7.154; ^{13}C: δ = 128.39) and $C_6D_5CHD_2$ (^1H: δ = 2.09; ^{13}C: δ = 20.40). Microanalyses were performed at the elemental analysis laboratory of the University of Duisburg-Essen. IR spectra were measured in an ALPHA-T FT-IR spectrometer equipped with a single reflection ATR sampling module. The melting points were measured using a Thermo Scientific 9300 apparatus.

Synthesis of $[L(Cl)Ga]_2PCl$ (1). LGa (250 mg, 0.513 mmol) and PCl_3 (35.22 mg, 22.43 µL, 0.256 mmol) were dissolved in 2 mL of toluene and stirred for 24 h, during which the color of the reaction solution changed from yellow to dark orange. Storage of the solution at -30 °C for 3 days yielded pale green solid of **1**. M. p. 230 °C. Yield 72.5 mg (25.4 %). Anal. Calcd. for $C_{58}H_{82}N_4Ga_2Cl_3P$: C, 62.64; H, 7.43; N, 5.04. Found: C, 62.6; H, 7.63; N, 5.33 %. ^1H NMR (600 MHz, [D8]Toluene, 25 °C): δ 7.10-6.93 (m, 6 H, C_6H_3-2,6-*i*Pr_2), 4.81 (s, 1 H, γ-C*H*), 3.55 (sept, 2 H, $^3J_{H\text{-}H}$ = 6.7 Hz, C*H*(CH_3)$_2$), 3.22 (sept, 2 H, $^3J_{H\text{-}H}$ = 6.8 Hz, C*H*(CH_3)$_2$), 1.46 (s, 6 H, ArNCC*H*$_3$), 1.21 (d, 6 H, $^3J_{H\text{-}H}$ = 6.8 Hz, CH(C*H*$_3$)$_2$), 1.18 (m, 12 H, $^3J_{H\text{-}H}$ = 6.6 Hz, CH(C*H*$_3$)$_2$), 0.98 (d, 6 H, $^3J_{H\text{-}H}$ = 6.8 Hz, CH(C*H*$_3$)$_2$). ^{13}C NMR (150 MHz, [D8]Toluene, 25 °C): δ 169.9 (ArN*C*CH$_3$), 145.6, 143.2, 142.1, 127.9, 127.5, 123.8 (Ar*C*), 98.2 (γ-CH), 29.5, 28.3 (*C*H(CH_3)$_2$), 27.4, 25.1, 24.6, 24.3 (CH(*C*H$_3$)$_2$), 24.0 (ArNC*C*H$_3$). ^{31}P NMR (242 MHz, [D8]Toluene, 25 °C): 0.52. IR (neat): ν 3063, 2965, 2925, 2866, 1521, 1461, 1437, 1382, 1314, 1254, 1177, 1099, 1018, 937, 865, 794, 757, 708, 639, 533, 474, 441, 399.

Synthesis of $[L(Br)Ga]_2PBr$ (2). LGa (100 mg, 0.205 mmol) and PBr_3 (27.77 mg, 9.74 µL, 0.103 mmol) were dissolved in 0.5 mL of toluene-d_8 in a J-Young NMR tube and stirred for 24 h, during which the color of the reaction solution changed from yellow to dark orange. Storage of the solution at -30 °C for 3 days yielded pale yellow crystals of **2**. M. p. 222 °C. Yield 48.3 mg (47.1 %). Anal. Calcd. for $C_{58}H_{82}N_4Ga_2Br_3P$: C, 55.93; H, 6.64; N, 4.50. Found: C, 56.10; H, 6.71; N, 4.71 %. ^1H NMR (500 MHz, [D8]Toluene, 25 °C): δ 6.98-6.91 (m, 6 H, C_6H_3-2,6-*i*Pr_2), 4.87 (s, 1 H, γ-C*H*), 3.63 (sept, 2 H, $^3J_{H\text{-}H}$ = 6.8 Hz, C*H*(CH_3)$_2$), 3.24 (sept, 2 H, $^3J_{H\text{-}H}$ = 6.8 Hz, C*H*(CH_3)$_2$), 1.47 (s, 6 H, ArNCC*H*$_3$), 1.25 (br d, 6 H, $^3J_{H\text{-}H}$ = 6.5 Hz, CH(C*H*$_3$)$_2$), 1.20 (br d, 12 H, $^3J_{H\text{-}H}$ = 6.8 Hz, CH(C*H*$_3$)$_2$), 0.96 (br d, 6 H, $^3J_{H\text{-}H}$ = 6.8 Hz, CH(C*H*$_3$)$_2$). ^{13}C NMR (125 MHz, [D8]Toluene, 25 °C): δ 169.9 (ArN*C*CH$_3$), 145.7, 143.3, 142.4, 127.6, 125.1, 123.7 (Ar*C*), 98.6 (γ-CH), 29.6, 28.4 (*C*H(CH_3)$_2$), 28.2, 25.1, 24.6, 24.5 (CH(*C*H$_3$)$_2$), 24.1 (ArNC*C*H$_3$). ^{31}P NMR (200 MHz, [D8]Toluene, 25 °C): -42.9. IR (neat): ν 2962, 2925, 2867, 1517, 1437, 1382, 1316, 1256, 1176, 1099, 1017, 935, 863, 797, 757, 639, 531, 450, 388.

Synthesis of $[L(Cl)Ga]_2As_2$ (3). LGa (100 mg, 0.205 mmol) and $AsCl_3$ (18.67 mg, 8.64 µL, 0.103 mmol) were dissolved in 0.5 mL of toluene-d_8 in a J-Young NMR tube and stirred for 24 h. During this period, the color of the reaction solution changed from yellow to reddish brown. The solution was kept at 0 °C for 1 day to yield green crystals of **3**. M. p. 255 °C (dec.). Yield 12.8 mg (10.7 %). Anal. Calcd. for $C_{58}H_{82}N_4Cl_2Ga_2As_2$: C, 58.27; H, 6.91; N, 4.69. Found: C, 58.12; H, 6.85; N, 4.55 %. ^1H NMR (500 MHz, [D8]Toluene, 25 °C): δ 7.08-6.89 (m, 6 H, C_6H_3-2,6-*i*Pr_2), 4.85(s, 1 H, γ-C*H*), 3.77 (sept, 2 H, $^3J_{H\text{-}H}$ = 6.8 Hz, C*H*(CH_3)$_2$), 2.90 (sept, 2 H, $^3J_{H\text{-}H}$ = 6.8 Hz, C*H*(CH_3)$_2$), 1.61 (s, 6 H, ArNCC*H*$_3$), 1.35 (d, 6 H, $^3J_{H\text{-}H}$ = 6.7 Hz, CH(C*H*$_3$)$_2$), 1.24 (d, 6 H, $^3J_{H\text{-}H}$ = 6.9 Hz, CH(C*H*$_3$)$_2$), 1.09 (d, 6 H, $^3J_{H\text{-}H}$ = 6.9 Hz, CH(C*H*$_3$)$_2$), 0.97 (d, 6 H, $^3J_{H\text{-}H}$ = 6.9 Hz, CH(C*H*$_3$)$_2$). ^{13}C NMR (125 MHz, [D8]Toluene, 25 °C): δ 169.1 (ArN*C*CH$_3$), 145.8, 142.7, 140.7, 127.4, 124.7, 124.1 (Ar*C*), 97.3 (γ-CH), 29.7, 28.0 (*C*H(CH_3)$_2$), 27.2, 24.8, 24.7, 23.9 (CH(*C*H$_3$)$_2$), 23.6 (ArNC*C*H$_3$). IR (neat): ν 3064, 2966, 2862, 1556, 1521, 1461, 1437, 1382, 1359, 1312, 1260, 1174, 1100, 1054, 1016, 935, 865, 790, 753, 711, 635, 526, 440.

Synthesis of $[L(Cl)Ga]As_2[Ga(NMe_2)L]$ (4). A solution of LGa (100 mg, 0.205 mmol) and Me_2NAsCl_2 (19.56 mg, 10.62 µL, 0.103 mmol) were dissolved in 0.5 mL of toluene-d_8 in a J-Young NMR tube and stirred for 24 h at 80 °C. The color of the reaction solution changed from yellow to red and a red solid precipitated, which was isolated by filtration and recrystallized in toluene, yielding reddish brown crystals of **4**. M. p. 239 °C. Yield 43.2 mg (34.8 %). Anal. Calcd. for $C_{60}H_{88}N_5Ga_2As_2Cl$: C, 59.85; H, 7.37; N, 5.82. Found: C, 60.06; H, 7.40; N, 6.04 %. ^1H NMR (600 MHz, [D8]Toluene, 25 °C): δ 7.11-6.86 (m, 12 H, C_6H_3-2,6-*i*Pr_2), 4.87 (s, 1 H, γ-C*H*), 4.72 (s, 1 H, γ-C*H*), 3.77 (sept, $^3J_{H\text{-}H}$ = 6.8 Hz, 2 H, C*H*(CH_3)$_2$), 3.54 (sept, $^3J_{H\text{-}H}$ = 6.8 Hz, 2 H, C*H*(CH_3)$_2$), 3.17 (sept, $^3J_{H\text{-}H}$ = 6.8 Hz, 2 H, C*H*(CH_3)$_2$), 2.95 (br s, 3 H, N(C*H*$_3$)$_2$), 2.77 (sept, $^3J_{H\text{-}H}$ = 6.8 Hz, 2 H, C*H*(CH_3)$_2$), 2.37 (br s, 3 H, N(C*H*$_3$)$_2$), 1.63 (s, 6 H, ArNCC*H*$_3$),1.60 (s, 6 H, ArNCC*H*$_3$), 1.31 (m, 18 H, $^3J_{H\text{-}H}$ = 6.8 Hz, CH(C*H*$_3$)$_2$), 1.21 (d, 6 H, $^3J_{H\text{-}H}$ = 6.8 Hz, CH(C*H*$_3$)$_2$), 1.13 (d, 6 H, $^3J_{H\text{-}H}$ = 6.8 Hz, CH(C*H*$_3$)$_2$), 1.02 (d, 6 H, $^3J_{H\text{-}H}$ = 6.8 Hz, CH(C*H*$_3$)$_2$), 0.98 (d, 6 H, $^3J_{H\text{-}H}$ = 6.8 Hz, CH(C*H*$_3$)$_2$), 0.97 (d, 6 H, $^3J_{H\text{-}H}$ = 6.8 Hz, CH(C*H*$_3$)$_2$). ^{13}C NMR (150 MHz, [D8]Toluene, 25 °C): δ 169.0, 168.4 (ArN*C*CH$_3$), 146.0, 145.1, 142.9, 142.5, 142.4, 141.3, 127.1, 127.0, 125.1, 124.5, 124.4, 123.7 (Ar*C*), 97.3, 96.3 (γ-CH), 44.8, 44.2 (N(*C*H$_3$)$_2$), 29.7, 29.2, 28.1, 28.0 (*C*H(CH_3)$_2$), 27.0, 25.8, 25.1, 24.8, 24.7, 24.5, 24.1 (CH(*C*H$_3$)$_2$), 23.7, 23.6 (ArNC*C*H$_3$). IR (neat): ν 2965, 2866, 2754, 1549, 1520, 1434, 1386, 1314, 1256, 1175, 1100, 1018, 975, 937, 856, 792, 754, 634, 546, 523, 856, 438 cm^{-1}.

Synthesis of $[(L(Me_2N)Ga]_2As_2$ (5). LGa (132 mg, 0.272 mmol) and $As(NMe_2)_3$ (28.12 mg, 25.00 µL, 0.136 mmol) were dissolved in 1.5 mL of mesitylene. The solution was stirred for 5 days at 165 °C. The color of the reaction solution changed from yellow to red and a red solid precipitated, which was isolated by filtration and washed with hexane, yielding a reddish orange solid of **5**. M. p. 248 °C (dec.). Yield 21.8 mg (13.3 %). Anal. Calcd. for $C_{62}H_{94}N_6Ga_2As_2$: C, 61.40; H, 7.81; N, 6.93. Found: C, 61.27; H, 7.82; N, 6.89 %. IR (neat): ν 3060, 2958, 2923, 2866, 2758, 1589, 1521, 1460, 1438, 1383, 1317, 1257, 1174, 1099, 1056, 1017, 975, 934, 885, 794, 757, 639, 600, 497, 478, 447 cm^{-1}.

Synthesis of $[L(Me_2N)Al]_2As_2$ (6). LAl (30 mg, 0.068 mmol) and $As(NMe_2)_3$ (6.98 mg, 6.21 µL 0.034 mmol) were dissolved in 0.5 mL of toluene-d_8 in a J-Young NMR tube and stirred for 4 h at 80 °C. The color of the reaction solution changed from red to reddish brown. The solution was kept at room temperature for further 3 days to yield pale yellow crystals of **6**. M. p. 275 °C. Yield 13 mg (35.6 %). Anal. Calcd. for $C_{62}H_{94}N_6Al_2As_2$: C, 66.06; H, 8.41; N, 7.46. Found: C, 65.88; H, 8.34; N, 7.51 %. ^1H NMR (500 MHz, [D8]Toluene, 25 °C): δ 7.12-6.94 (m, 6 H, C_6H_3-2,6-*i*Pr_2), 4.92 (s, 1 H, γ-C*H*), 3.53 (sept, $^3J_{H\text{-}H}$ = 6.8 Hz, 2 H, C*H*(CH_3)$_2$), 2.93 (sept, $^3J_{H\text{-}H}$ = 6.8 Hz, 2 H, C*H*(CH_3)$_2$), 2.69 (s, 3 H, N(C*H*$_3$)$_2$), 2.36 (s, 3 H, N(C*H*$_3$)$_2$), 1.61 (s, 6 H, ArNCC*H*$_3$), 1.28 (m, 12 H, CH(C*H*$_3$)$_2$), 0.99 (d, 6 H, $^3J_{H\text{-}H}$ = 6.8 Hz, CH(C*H*$_3$)$_2$), 0.96 (d, 6 H, $^3J_{H\text{-}H}$ = 6.8 Hz, CH(C*H*$_3$)$_2$). ^{13}C NMR (150 MHz, [D8]Toluene, 25 °C): δ 169.4 (ArN*C*CH$_3$), 145.4, 143.2, 142.1, 126 .9, 124.4, 124.2 (Ar*C*), 98.0 (γ-CH), 44.2, 42.5 (N(*C*H$_3$)$_2$), 29.2, 28.1 (*C*H(CH_3)$_2$), 25.8, 25.2, 24.8, 24.7 (CH(*C*H$_3$)$_2$), 23.7 (ArNC*C*H$_3$). IR (neat): ν 2962, 2866, 2758, 1622, 1521, 1435, 1389, 1314, 1257, 1166, 1092, 1014, 980, 935, 865, 790, 758, 711, 642, 619, 544, 524, 428 cm^{-1}.

Synthesis of $[L(Et_2N)Ga]_2Bi_2$ (7). $Bi(NEt_2)_3$ (0.066 g, 45 µL, 0.15 mmol) was added to a solution of LGa (0.15 g, 0.30 mmol) in 3 mL of toluene at ambient temperature. The solution was stirred for 4 days, during which the color changed from yellow to purple. Storage of the solution at ambient temperature for 2 days resulted in the formation of purple crystals of **7**,

which were washed with hexane (2x1 mL) to afford **7** in a pure form. M. p. 120 °C (dec.). Yield 0.083 g (65 %). Anal. Calcd. for $C_{66}H_{102}Bi_2Ga_2N_6$: C, 51.58; H, 6.69; N, 5.47. Found: C, 51.76; H, 6.61; N, 5.42 %. ^{1}H NMR (600 MHz, [D$_6$]Benzene, 25 °C): δ 7.11 (m, 6 H, Ar*H*), 7.00 (m, 6 H, Ar*H*), 4.74 (s, 2 H, γ-C*H*), 4.07 (sept, $^3J_{HH}$ = 6.8 Hz, 4 H, C*H*(CH$_3$)$_2$), 3.72 (q, $^3J_{HH}$ = 6.9 Hz, 4 H, NC*H*$_2$CH$_3$), 2.80 (q, $^3J_{HH}$ = 6.9 Hz, 4 H, NC*H*$_2$CH$_3$), 2.77 (sept, $^3J_{HH}$ = 6.8 Hz, 4 H, C*H*(CH$_3$)$_2$), 1.58 (s, 12 H, ArNCC*H*$_3$), 1.39 (d, $^3J_{HH}$ = 6.8 Hz, 12 H, CH(C*H*$_3$)$_2$), 1.36 (t, $^3J_{HH}$ = 6.9 Hz, 6 H, NCH$_2$C*H*$_3$), 1.29 (d, $^3J_{HH}$ = 6.8 Hz, 12 H, CH(C*H*$_3$)$_2$), 1.11 (d, $^3J_{HH}$ = 6.8 Hz, 12 H, CH(C*H*$_3$)$_2$), 1.05 (d, $^3J_{HH}$ = 6.8 Hz, 12 H, CH(C*H*$_3$)$_2$), 1.02 (br s, 6 H, NCH$_2$C*H*$_3$). ^{13}C NMR (150 MHz, [D$_6$]Benzene, 25 °C). δ 169.1 (ArN*C*CH$_3$), 145.7, 143.7, 143.4, 143.4, 127.0, 125.4, 124.6 (Ar*C*), 98.3 (γ-*C*H), 48.1, 46.4 (N*C*H$_2$CH$_3$), 29.3, 27.5, (*C*H(CH$_3$)$_2$), 27.1 (CH(*C*H$_3$)$_2$), 25.6 (ArNC*C*H$_3$), 24.8 (CH(*C*H$_3$)$_2$), 17.9, 16.4 (NCH$_2$*C*H$_3$). IR (neat): ν 2962, 2923, 2864, 2818, 1543, 1517, 1461, 1438, 1383, 1313, 1254, 1168, 1104, 1057, 1008, 935, 876, 853, 793, 757, 719, 625, 593, 559, 530, 456, 438 cm^{-1}.

Computational details. The geometric parameters of the species under study were fully optimized in the gas phase at the BP86-D3/def2-SVP theoretical level[27–30] with a corresponding small-core relativistic effective core potential for Sb and Bi[31] employing ultrafine grid. The stationary points were characterized as minima on the potential energy surface by vibrational analysis (the number of imaginary frequencies (NImag) was equal to zero) and the structures obtained were used for the subsequent calculations. AIM[32] and ELF[33,34] computations were performed with DGrid program[42] using densities from the all-electron scalar relativistic (SR) ZORA-BP86-D3/TZP computations.[27–29,43] ELF basin populations were calculated for a rectangular parallelepipedic grid with a mesh size of 0.1 bohr. The energies of frontier molecular orbitals were calculated at the ωB97X-D/def2-SVP level of theory.[44] NBO analysis[35] was performed at the BP86-D3/def2-SVP theoretical level as implemented in Gaussian09.[45] SR-ZORA-BP86-D3/TZP computations were performed using ADF2013 suite of programs (core potentials were not used, and quality of the Becke numerical integration grid was set to the keyword *good*),[46–48] while the remaining computations were carried out in Gaussian09 code.[45] Detailed information about AIM, ELF, and NBO can be found elsewhere.[32–35]

Single-crystal X-ray analyses. The crystals were mounted on nylon loops (**2·2C$_7$H$_8$**, **3**, **4**, **6**) and a glass fiber (**7**) in inert oil. Data were collected using a Bruker AXS D8 Kappa diffractometer with APEX2 detector (mono-chromated Mo$_{K\alpha}$ radiation, λ = 0.71073 Å) at 100(2)K (**2·2C$_7$H$_8$**, **3**, **6**) and 170(2)K (**4**) and a STOE IPDS II (mono-chromated Mo$_{K\alpha}$ radiation, λ = 0.71073 Å) at 173(2)K (**7**). **2·2C$_7$H$_8$**: [$C_{72}H_{98}Br_3Ga_2N_4P$·2C_7H_8], M = 1429.68, pale yellow crystal, (0.390 × 0.329 × 0.160 mm); monoclinic, space group $P2_1/c$; a = 14.1855(7) Å, b = 20.0810(9) Å, c = 24.7875(12) Å; α = 90°, β = 99.843(3)°, γ = 90°, V = 6957.0(6) Å^3; Z = 4; μ = 2.563 mm^{-1}; ρ_{calc} = 1.365 g·cm^{-3}; 176583 reflections (θ_{max} = 33.295°), 26734 unique (R_{int} = 0.0425); 955 parameters; largest max./min in the final difference Fourier synthesis 2.178 e·Å^{-3}/ -1.654 e·Å^{-3}; max./min. transmission 0.61/0.30; R_1 = 0.0571 (I > 2σ(I)), wR_2 = 0.1386 (all data). **3**: [$C_{58}H_{82}As_2Cl_2Ga_2N_4$], M = 1195.45, greenish yellow crystal, (0.116 × 0.050 × 0.046 mm); monoclinic, space group $P2_1/n$; a = 13.6550(16) Å, b = 13.9479(15) Å, c = 15.7645(19) Å; α = 90°, β = 105.410(4)°, γ = 90°, V = 2894.5(6) Å^3; Z = 2; μ = 2.197 mm^{-1}; ρ_{calc} = 1.372 g·cm^{-3}; 34154 reflections (θ_{max} = 30.503°), 8734 unique (R_{int} = 0.0512); 317 parameters; largest max./min in the final difference Fourier synthesis 0.589 e·Å^{-3}/ -0.737 e·Å^{-3}; max./min. transmission 0.75/0.70; R_1 = 0.0489 (I > 2σ(I)), wR_2 = 0.0965 (all data). **4**:·[$C_{60}H_{88}As_2ClGa_2N_5$], M = 1204.08, brownish orange crystal, (0.200 × 0.200 × 0.100 mm); triclinic, space group P-1; a = 10.7219(8) Å, b = 12.2486(8) Å, c = 13.2240(9) Å; α = 93.277(6)°, β = 107.628(6)°, γ = 108.982(6)°, V = 1541.6(2) Å^3; Z = 1; μ = 2.021 mm^{-1}; ρ_{calc} = 1.297 g·cm^{-3}; 14495 reflections (θ_{max} = 26.369°), 6281 unique (R_{int} = 0.0475); 347 parameters; largest max./min in the final difference Fourier synthesis 0.648 e·Å^{-3}/ -0.477 e·Å^{-3}; max./min. transmission 1.00000/0.89851; R_1 = 0.0465 (I > 2σ(I)), wR_2 = 0.1173 (all data). **6**:·[$C_{62}H_{94}Al_2As_2N_6$], M = 1127.23, pale yellow crystal, (0.401 × 0.327 × 0.040 mm); triclinic, space group P-1; a = 10.7453(7) Å, b = 15.6155(10) Å, c = 18.2991(12) Å; α = 84.315(3)°, β = 89.408(3)°, γ = 79.142(3)°, V = 3000.6(3) Å^3; Z = 2; μ = 1.186 mm^{-1}; ρ_{calc} = 1.248 g·cm^{-3}; 72834 reflections (θ_{max} = 30.694°), 18296 unique (R_{int} = 0.0426); 673 parameters; largest max./min in the final difference Fourier synthesis 1.581 e·Å^{-3}/ -0.874 e·Å^{-3}; max./min. transmission 0.75/0.58; R_1 = 0.0473 (I > 2σ(I)), wR_2 = 0.1432 (all data). **7**: [$C_{66}H_{102}Bi_2Ga_2N_6$], M = 1536.93, red crystal, (0.250 × 0.150 × 0.120 mm); monoclinic, space group $P2_1/n$; a = 11.4654(3) Å, b = 14.0433(3) Å, c = 20.8486(4) Å; α = 90°, β = 90.352(2)°, γ = 90°, V = 3356.81(13) Å^3; Z = 2; μ = 6.062 mm^{-1}; ρ_{calc} = 1.521 g·cm^{-3}; 51838 reflections (θ_{max} = 26.000°), 6597 unique (R_{int} = 0.0856); 375 parameters; largest max./min in the final difference Fourier synthesis 1.004 e·Å^{-3}/ -1.223 e·Å^{-3}; max./min. transmission 0.274/0.184; R_1 = 0.0499 (I > 2σ(I)), wR_2 = 0.0859 (all data). The structures were solved by Direct Methods (SHELXS-97)[49] and refined anisotropically by full-matrix least-squares on F^2 (SHELXL-2014).[50] Absorption corrections were performed semi-empirically from equivalent reflections on basis of multi-scans (**4**, **6**, **7**) or numerical from indexed faces (**2·2C$_7$H$_8$**) (SABABS, XPREP). Hydrogen atoms were refined using a riding model or rigid methyl groups. In **2** the central P-Br group is disordered over three position. The P-Br distances were restrained to be equal (SADI) and RIGU restraints were applied to the ADP. The P atom of the smallest component could only be refined isotropically. An iso-propyl group is disordered over two position. The bond lengths of corresponding bonds were restrained to be equal and RIGU, SIMU and DELU restraints were applied to the ADP of the C atoms. The structure also contains two toluene molecules, which are disordered over two positions each. The fragments were fitted with DSR[51] and SADI restraints were use for the 1,2 and 1,3 distances. The C-C bond of the methyl group was restrained to be 1.51 Å (DFIX) and the entire molecules were restrained to planarity (FLAT). SIMU and RIGU restraints were applied to the ADP. In **4** the molecule is disordered over a center of inversion. A refinement in P1 resolves the disorder but leads to serious problems with correlations and unrealistic values of the bonding parameter of the NMe$_2$ residue. RIGU restraints were applied to the ADP of the NMe$_2$ group. One of the ethyl groups of the diethylamido ligand of **7** is disordered. Appropriate distance and anisotropic displacement restraints were used for this fragment.

The crystallographic data of **2·2C$_7$H$_8$**, **3**, **4**, **6** and **7** (excluding structure factors) have been deposited with the Cambridge Crystallographic Data Centre as supplementary publication nos. CCDC-1579373 (**2**), CCDC-1583617 (**3**), CCDC-1579371 (**4**), CCDC-1579372 (**6**) and CCDC-579351 (**7**). Copies of the data can be obtained free of charge from The Cambridge Crystallographic Data Centre via www.ccdc.cam.ac.uk/data_request/cif.

Acknowledgements

St.S. acknowledges financial support by the Deutsche Forschungsgemeinschaft DFG (SCHU 1069/22-1) and A.S.N. is thankful to the Siberian Supercomputer Center SB RAS for providing computational resources. Dr. K. Merz (Ruhr University Bochum) and E. Hammes (University of Düsseldorf) are acknowledged for data collection (XRD) of compounds **2** and **7**.

Keywords: Main group elements • Subvalent compounds • Bond activation reaction

[1] **Reviews**: a) C. Jones, A. Stasch In *The Group 13 Metals Aluminium, Gallium, Indium and Thallium: Chemical Patterns and Peculiarities*, Chapter 5, Eds. S. Aldridge, A. J. Downs, **2011**, John Wiley & Sons; b)

Y.-C. Tsai, *Coord. Chem. Rev*. **2012**, *256*, 722–758; c) M. Asay, C. Jones, M. Driess, *Chem. Rev*. **2011**, *111*, 354–396; d) S. Nagendran, H. W. Roesky, Organometallics **2008**, *27*, 457–492; e) R. J. Baker, C. Jones, *Coord. Chem. Rev*. **2005**, *249*, 1857–1869; f) S. Gonzalez-Gallardo, G. Prabusankar, T. Cadenbach, C. Gemel, M. von Hopffgarten, G. Frenking, R. A. Fischer, *Struct. Bonding* (Berlin) **2010**, *136*, 147–188.

[2] N. J. Hardman, P. P. Power, *ACS Symp. Ser*. **2002**, *822*, 2–15

[3] H. W. Roesky, In *Inorganic Chemistry in Focus II*; Eds. G. Meyer, D. Naumann, L. Wesemann, Wiley-VCH, Weinheim, Germany, **2005**, pp 89–103.

[4] T. Chu, I. Korobkov, G. I. Nikonov, *J. Am. Chem. Soc*. **2014**, *136*, 9195–9202

[5] a) T. Chu, Y. Boyko, I. Korobkov, G. I. Nikonov, *Organometallics* **2015**, *34*, 5363–5365; b) M. R. Crimmin, M. J. Butler, A. J. P. White, *Chem. Commun*. **2015**, *51*, 15994–15996; c) L. Kong, R. Ganguly, Y. Li, R. Kinjo, *Chem. Eur. J*. **2016**, *22*,1922–1925.

[6] a) N. Hardman, R. J. Wright, A. D. Philips, P. P. Power, *J. Am. Chem. Soc*. **2003**, *125*, 2667–2679; b) A. Kempter, C. Gemel, N.J. Hardman, R. A. Fischer, *Inorg. Chem*. **2006**, *45*, 3133–3138; c) A. Kempter, C. Gemel, R. A. Fischer, *Chem. Commun*. **2006**, 1551–1553; d) A. Kempter, C. Gemel, T. Cadenbach, R. A. Fischer, *Organometallics* **2007**, *26*, 4257–4264; e) A. Kempter, C. Gemel, R. A. Fischer, *Chem. Eur. J.* **2007**, *13*, 2990–3000.

[7] a) A. Seifert, D. Scheid, G. Linti, T. Zessin, *Chem. Eur. J*. **2009**, *15*, 12114–12120; b) E. Herappe-Mejía, K. Trujillo-Hernández, J. Carlos Garduño-Jiménez, F. Cortés-Guzmán, D. Martínez-Otero, V. Jancik, *Dalton Trans*. **2015**, *44*, 16894–16902.

[8] A. Kempter, C. Gemel, R. A. Fischer, *Inorg. Chem*. **2008**, *47*, 7279–7285.

[9] G. Prabusankar, C. Gemel, M. Winter, R. W. Seidel, R. A. Fischer, *Chem. Eur. J.* **2010**, *16*, 6041–6047.

[10] G. Prabusankar, A. Kempter, C. Gemel, M.-K. Schröter, R. A. Fischer, *Angew. Chem.* **2008**, *120*, 7344–7347; *Angew. Chem. Int. Ed*. **2008**, *47*, 7234–7237.

[11] G. Prabusankar, C. Gemel, P. Parameswaran, C. Flener, G. Frenking. R. A. Fischer, *Angew. Chem.* **2009**, *121*, 5634–5637; *Angew. Chem. Int. Ed*. **2009**, *48*, 5526–5529.

[12] A. Doddi, C. Gemel, M. Winter, R. A Fischer, C. Goedecke, H. S. Rzepa, G. Frenking, *Angew. Chem*. **2013**, *125*, 468–472; *Angew. Chem. Int. Ed.* **2013**, *52*, 450–454.

[13] C. Ganesamoorthy, D. Bläser, C. Wölper, S. Schulz, *Chem. Commun.* **2014**, *50*, 12382–12384.

[14] a) L. Tuscher, C. Ganesamoorthy, D. Bläser, C. Wölper, S. Schulz, *Angew. Chem.* **2015**, *127*, 10803–10807; *Angew. Chem. Int. Ed.* **2015**, *54*, 10657–10661; b) L. Tuscher, C. Helling, C. Ganesamoorthy, J. Krüger, C. Wölper, W. Frank, A. S. Nizovtsev, S. Schulz, *Chem. Eur. J.* **2017**, *23*, 12297–12304.

[15] C. Ganesamoorthy, D. Bläser, C. Wölper, S. Schulz, *Angew. Chem.* **2014**, *126*, 11771–11775; *Angew. Chem. Int. Ed.* **2014**, *53*, 11587–11591.

[16] T. Chu, Y. Boyko, I. Korobkov, L. G. Kuzmina, J. A. K. Howard, G. I. Nikonov, *Inorg. Chem.* **2016**, *55*, 9099–9104.

[17] C. Ganesamoorthy, J. Krüger, C. Wölper, A. S. Nizovtsev, S. Schulz, *Chem. Eur. J*. **2017**, *23*, 2461–2468.

[18] C. Ganesamoorthy, C. Wölper, A. S. Nizovtsev, S. Schulz, *Angew. Chem.* **2016**, *128*, 4276–4281; *Angew. Chem. Int. Ed.* **2016**, *55*, 4204–4209.

[19] J. K. West, L. Stahl, *Inorg. Chem*. **2017**, *56*, 12728–12738.

[20] See for instance: a) L. Weber, *Chem. Rev*. **1992**, *92*, 1839–1906; b) L. Weber, K. Reizig, D. Bungardt, R. Boese, *Organometallics* **1987**, *6*, 110–114; c) J. Grobe, D. L. van, T. Pohlmeyer, B. Krebs, O. Conrad, E. Dobbert, L. Weber, *Organometallics* **1998**, *17*, 3383–3386; d) L. Weber, H. Bastian, A. Müller, H. Boegge, *Z. Naturforsch. B* **1992**, *47*, 231–237; e) L. Weber, M. Frebel, R. Boese, *Organometallics* **1989**, *8*, 1718–1722; f) W. Domańska-Babul, J. Chojnacki, E. Matern, J. Pikies, *J. Organomet. Chem*. **2007**, *692*, 3640–3648.

[21] a) L. Liu, D. A. Ruiz, F. Dahcheh, G. Bertrand, R. Suter, A. M. Tondreau, H. Grützmacher, *Chem. Sci*. **2016**, *7*, 2335–2341; b) E. B. Hulley, P. T. Wolczanski, E. B. Lobkovsky, *Chem. Comm*. **2009**, 6412–6414.

[22] a) S. Heinl, S. Reisinger, C. Schwarzmaier, M. Bodensteiner, M. Scheer, *Angew. Chem.* **2014**, *126*, 7769–7773; *Angw. Chem. Int. Ed*. **2014**, *53*, 7639–7642; b) E. Niecke, R. Rüger, B. Krebs, *Angew. Chem.* **1982**, *94*, 553–554*; Angew. Chem. Int. Ed.* **1982**, *21*, 544–545; c) R. Riedel, H.-D. Hausen, E. Fluck, *Angew. Chem.* **1985**, *97*, 1050-1051*; Angew. Chem. Int. Ed.* **1985**, *24*, 1056–1057.

[23] Cambridge Structural Database V5.38 (update May 2017); see also: F. H. Allen, *Acta Crystallogr*., *Sect. B: Struct. Sci*. **2002**, *B58*, 380–388. Nine hits, coordination number of As restricted to 2, any atom bonded to As, As-As bonds defined as type "double bond".

[24] P. Pyykkö, M. Atsumi, *Chem. Eur. J*. **2009**, *15*, 186–197.

[25] M. Rahm, R. Hoffmann, N. W. Ashcroft, *Chem. Eur. J*. **2016**, *22*, 14625–14632.

[26] Cambridge Structural Database V5.38 (update May 2017); see also: F. H. Allen, *Acta Crystallogr*., *Sect. B: Struct. Sci*. **2002**, *B58*, 380–388. 13 hits, coordination number of Bi restricted to 2, any atom bonded to Bi, Bi-Bi bonds defined as type "double bond".

[27] A. D. Becke, *Phys. Rev. A* **1988**, *38*, 3098–3100.

[28] J. P. Perdew, *Phys. Rev. B* **1986**, *33*, 8822–8824.

[29] S. Grimme, J. Antony, S. Ehrlich, H. Krieg, *J. Chem. Phys.* **2010**, *132*, 154104.

[30] F. Weigend. R. Ahlrichs, *Phys. Chem. Chem. Phys.* **2005**, *7*, 3297–3305.

[31] B. Metz, H. Stoll, M. Dolg, *J. Chem. Phys.* **2000**, *113*, 2563–2569.

[32] R. F. W Bader. Atoms in Molecules: A Quantum Theory, Claredon Press: Oxford, U.K., 1990.

[33] A. D. Becke, K. E. Edgecombe, *J. Chem. Phys.* **1990**, *92*, 5397–5403.

[34] B. Silvi, A. Savin, *Nature* **1994**, *371*, 683–686.

[35] A. E. Reed, L. A. Curtiss, F. Weinhold, *Chem. Rev.* **1988**, *88*, 899–926.

[36] A. S. Nizovtsev, A. S. Ivanov, A. I. Boldyrev, S. N. Konchenko, *Eur. J. Inorg. Chem*. **2015**, 5801–5807.

[37] S. Raub, G. Jansen, *Theor. Chem. Acc.* **2001**, *106*, 223–232.

[38] N. J. Hardman, B. E. Eichler, P. P. Power, *Chem. Commun*. **2000**, 1991–1992.

[39] C. Cui, H. W. Roesky, H.-G. Schmidt, M. Noltemeyer, H. Hao, F. Cimpoesu, *Angew. Chem.* **2000**, *112*, 4444-4446; *Angew. Chem. Int. Ed.* **2000**, *39*, 4274-4276.

[40] H. Schumann, *J. Organomet. Chem.* **1986**, *299*, 168-178.

[41] V. Vehkamäki, T. Hatanpää, M. Ritala, M. Leskelä, *J. Mater. Chem.* **2004**, *14*, 3191–3197.

[42] M. Kohout, DGrid, version 4.6, Radebeul, 2011.

[43] E. van Lenthe, R. van Leeuwen, E. J. Baerends, *Int. J. Quantum Chem.* **1996**, *57*, 281–293.

[44] J.-D. Chai, M. Head-Gordon, *Phys. Chem. Chem. Phys.*, **2008**, *10*, 6615–6620.

[45] M. J. Frisch, G. W. Trucks, H. B. Schlegel, G. E. Scuseria, M. A. Robb, J. R. Cheeseman, G. Scalmani, V. Barone, B. Mennucci, G. A. Petersson, H. Nakatsuji, M. Caricato, X. Li, H. P. Hratchian, A. F. Izmaylov, J. Bloino, G. Zheng, J. L. Sonnenberg, M. Hada, M. Ehara, K. Toyota, R. Fukuda, J. Hasegawa, M. Ishida, T. Nakajima, Y. Honda, O. Kitao, H. Nakai, T. Vreven, J. A. Montgomery, Jr., J. E. Peralta, F. Ogliaro, M. Bearpark, J. J. Heyd, E. Brothers, K. N. Kudin, V. N. Staroverov, R. Kobayashi, J. Normand, K. Raghavachari, A. Rendell, J. C. Burant, S. S. Iyengar, J. Tomasi, M. Cossi, N. Rega, J. M. Millam, M. Klene, J. E. Knox, J. B. Cross, V. Bakken, C. Adamo, J. Jaramillo, R. Gomperts, R. E. Stratmann, O. Yazyev, A. J. Austin, R. Cammi, C. Pomelli, J. W. Ochterski, R. L. Martin, K. Morokuma, V. G. Zakrzewski, G. A. Voth, P. Salvador, J. J. Dannenberg, S. Dapprich, A. D. Daniels, Ö. Farkas, J. B. Foresman, J. V. Ortiz, J. Cioslowski, D. J. Fox, Gaussian 09, Revision D.01; Gaussian, Inc.: Wallingford CT, 2013.

[46] ADF2013, SCM, Theoretical Chemistry, Vrije Universiteit, Amsterdam, The Netherlands, http://www.scm.com.

[47] C. F. Guerra, J. G. Snijders, G. te Velde, E. J. Baerends, *Theor. Chem. Acc.*, **1998**, *99*, 391–403.

[48] G. te Velde, F. M. Bickelhaupt, E. J. Baerends, C. Fonseca Guerra, S. J. van Gisbergen, J. G. Snijders, T. Ziegler, *J. Comput. Chem.*, **2001**, *22*, 931–967.

[49] G. M. Sheldrick, *Acta Crystallogr.* **1990**, *A46*, 467–473

[50] G. M. Sheldrick, SHELXL-2014, Program for the Refinement of Crystal Structures University of Göttingen, Göttingen (Germany) **2014** (see also: G. M. Sheldrick, *Acta Crystallogr.* **2008**, *A64*, 112–122). shelXle, *A Qt GUI for SHELXL*, C. B. Hübschle, G. M. Sheldrick, B. Dittrich, *J. Appl. Cryst.* **2011**, *44*, 1281–1284.

[51] D. Kratzert, J. J. Holstein, I. Krossing, *J. Appl. Cryst.* **2015**, *48*, 933–938.

Entry for the Table of Contents

FULL PAPER

LGa reacted with PX_3 with formation of $[L(X)Ga]_2PX$ (X = Cl **1**, Br **2**), whereas reactions with $AsCl_3$, Me_2NAsCl_2, $As(NMe_2)_3$ and $Bi(NEt_2)_3$ yielded Ga-substituted dipnictenes $[L(Cl)Ga]_2As_2$ (**3**), $[L(Cl)Ga]_2As_2[Ga(NMe_2)L]$ (**4**), $[L(Me_2N)Ga]_2As_2$ (**5**) and $[L(Cl)Ga]_2Bi_2$ (**7**). The stronger reductant LAl reacted with $As(NMe_2)_3$ under milder conditions with formation of $[L(Me_2N)Al]_2As_2$ (**6**). Quantum chemical calculations revealed the bonding situation within **4**, **6** and **7**.

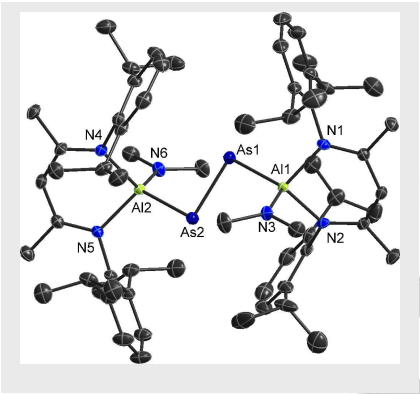

*L. Tuscher, C. Helling, C. Wölper, W. Frank, A. S. Nizovtsev, and S. Schulz**

Page No. – Page No.

A general route to metal-substituted dipnictenes of the type $[L(X)M]_2E_2$ (M = Al, Ga; E = As, Bi; X = halide, amide)

DOI: 10.1002/chem.201705233
URN: urn:nbn:de:hbz:464-20201215-110613-5

This is the peer reviewed version of the following article: Tuscher, L., Helling, C., Wölper, C., Frank, W., Nizovtsev, A.S., Schulz, S.: A General Route to Metal-Substituted Dipnictenes of the Type [L(X)M]2E2. Chemistry - A European Journal 2018, 24, 3241-3250, which has been published in final form at: https://doi.org/10.1002/chem.201705233